doi:10.1093/plphys/kiab262 PLANT PHYSIOLOGY 2021: 187: 378–395

Plant Physiology®

Research Article

Downsizing in plants—UV light induces pronounced morphological changes in the absence of stress

Minjie Qian [1,2] Eva Rosenqvist [3] Els Prinsen [4] Frauke Pescheck [5] Ann-Marie Flygare,[6] Irina Kalbina [1] Marcel A.K. Jansen [7] and Åke Strid [1,*,†]

1 Örebro Life Science Center, School of Science and Technology, Örebro University, SE-70182 Örebro, Sweden
2 College of Horticulture, Hainan University, Haikou 570228, China
3 Section of Crop Sciences, Department of Plant and Environmental Sciences, University of Copenhagen, Højbakkegård Allé 9, DK-2630 Taastrup, Denmark
4 Integrated Molecular Plant Physiology Research, Department of Biology, University of Antwerpen, Groenenborgerlaan 171, B-2020 Antwerpen, Belgium
5 Botanical Institute, Christian-Albrechts-University Kiel, Olshausenstraße 40, 24098 Kiel, Germany
6 Statistics Unit, School of Business, Örebro University, SE-70182 Örebro, Sweden
7 School of Biological, Earth and Environmental Sciences, Environmental Research Institute, University College Cork, North Mall, T23 TK30 Cork, Ireland

*Author for communication: ake.strid@oru.se
†Senior author.

Å.S., M.A.K.J., E.R., M.Q. and I.K. planned the research. M.Q., Å.S., M.A.K.J., E.R., E.P., and F.P. designed the experiments. M.Q., E.P., F.P., and I.K. performed the experiments. M.Q., E.P., Å.S., F.P., A.-M.F., E.R., and M.A.K.J. analyzed the data. Å.S. and M.A.K.J. wrote the paper with contributions from M.Q., E.R., A.-M.F., E.P., and F.P. All authors commented and approved the manuscript.
The author responsible for distribution of materials integral to the findings presented in this article in accordance with the policy described in the Instruction for Authors (https://academic.oup.com/plphys/pages/general-instructions) is: Åke Strid (ake.strid@oru.se)

Abstract

Ultraviolet (UV) light induces a stocky phenotype in many plant species. In this study, we investigate this effect with regard to specific UV wavebands (UV-A or UV-B) and the cause for this dwarfing. UV-A- or UV-B-enrichment of growth light both resulted in a smaller cucumber (*Cucumis sativus* L.) phenotype, exhibiting decreased stem and petiole lengths and leaf area (LA). Effects were larger in plants grown in UV-B- than in UV-A-enriched light. In plants grown in UV-A-enriched light, decreases in stem and petiole lengths were similar independent of tissue age. In the presence of UV-B radiation, stems and petioles were progressively shorter the younger the tissue. Also, plants grown under UV-A-enriched light significantly reallocated photosynthates from shoot to root and also had thicker leaves with decreased specific LA. Our data therefore imply different morphological plant regulatory mechanisms under UV-A and UV-B radiation. There was no evidence of stress in the UV-exposed plants, neither in photosynthetic parameters, total chlorophyll content, or in accumulation of damaged DNA (cyclobutane pyrimidine dimers). The abscisic acid content of the plants also was consistent with non-stress conditions. Parameters such as total leaf antioxidant activity, leaf adaxial epidermal flavonol content and foliar total UV-absorbing pigment levels revealed successful UV acclimation of the plants. Thus, the UV-induced dwarfing, which displayed different phenotypes depending on UV wavelengths, occurred in healthy cucumber plants, implying a regulatory adjustment as part of the UV acclimation processes involving UV-A and/or UV-B photoreceptors.

Received February 26, 2021. Accepted May 18, 2021. Advance access publication June 7, 2021

Introduction

The study of plant ultraviolet (UV) responses has gradually shifted from plant stress biology into the realm of plant regulatory responses (Jansen and Bornman, 2012). There is now a good, emerging understanding of the mechanism underlying the sensing of UV-B and UV-A wavelengths by a range of dedicated plant photoreceptors, including the phototropins, cryptochromes, and UV RESISTANCE LOCUS 8 (UVR8) (Paik and Huq, 2019). However, understanding of downstream regulatory interactions which can substantially modify UV-A and UV-B responses is only slowly emerging. Nevertheless, there is consensus that both UV-B and UV-A signaling pathways closely interact (Rai et al., 2019, 2020), with further crosstalk with, among others, phytochrome signaling. For example, UV-B through UVR8 accelerates degradation of PHYTOCHROME INTERACTING FACTORS (PIFs) that are part of the phytochrome-mediated elongation response to high far-red to red light ratio's (Sharma et al., 2019). As a consequence of these interactions, plant responses under natural light conditions are not always identical to those observed under controlled, artificial lighting in the laboratory. For example, Morales et al. (2013) showed that under natural sunlight, UVR8 both positively and negatively affects UV-A-regulated gene expression and metabolite accumulation. Conversely, a high UV-A/blue light background radiation moderates UV-B-driven gene-expression.

Understanding plant UV responses under natural conditions is particularly important in the context of climate change. Ongoing changes in the global climate, recovery of the stratospheric ozone layer, and interactions between these two processes are resulting in novel combinations of, among others, temperature, water availability, and solar UV radiation (Bornman et al., 2019). For example, plants in the Mediterranean are predicted to be exposed to higher UV levels, due to climate change-associated changes in cloud cover, together with increased spells of drought (Bornman et al., 2019). It has been hypothesized that UV-exposed plants will be more drought-protected. Indeed, Robson et al. (2015a) showed that when *Betula pendula* (silver birch) seedlings were exposed to a combination of natural UV and drought, wilting was less pronounced compared with that in plants which had just been exposed to drought. However, not all studies show such cross-tolerance (Rodríguez-Calzada et al., 2019), and there is still considerable uncertainty in the literature concerning the environmental relevance of cross-tolerance (Jansen et al., 2019). Nevertheless, it has been argued that a key component of any putative cross-tolerance is the UV-induced change in plant architecture, and especially a stockier phenotype. The UV-induced phenotype is characterized by shorter stems, internodes, and petioles, and a diminished leaf area (LA), often associated with an increase in leaf thickness (Jansen et al., 1998; Robson et al., 2015b), and some of these characteristics are shared with drought-acclimated plants. Yet, major questions remain concerning the stocky UV phenotype, and particularly the mechanism underlying the induction of such a phenotype. UV-induced stress, possibly involving reactive oxygen species (ROS; Hideg et al., 2013) and/or accumulation of damaged DNA (Kang et al., 1998), may affect plant architecture (Robson et al., 2015b). Conversely, a regulatory response mediated by a UV photoreceptor can drive architectural change. In the latter case, UV-B- and UV-A-induced responses may be different as these are driven by distinct photoreceptors.

The aim of the current study was to investigate whether morphological changes occurred in plants as a result of supplementing photosynthetically active radiation (PAR) with additional UV-A- or UV-B-enriched light, and to ascertain if such alteration is due to known UV-induced stress factors such as reduction of photosynthetic capacity (Jordan et al., 2016), ROS formation (Hideg et al., 2013), DNA damage (Kalbin et al., 2001), or changes in hormonal status (Hideg and Strid, 2017). The study was carried out in cucumber (*Cucumis sativus* L.), a model species representing broad leaved, high biomass plants of considerable economic importance and which develops considerable phenotypic changes dependent on different wavelengths of UV light (Ballaré et al., 1991).

Results

A more dwarfed, UV-induced, plant architecture has been observed in many different plant species, following exposure to UV radiation. However, some of the strongest morphological responses have been observed in cucumber (e.g. see Qian et al., 2020). In the present study, we analyzed the induction of a more dwarfed architecture in cucumber cv Hi Jack. Two-week-old cucumber plants were exposed to UV light for 14 days, during which the stem length of control plants increased from, on average, 4.1 to 47.9 cm. Plants exposed to UV-A- or UV-B-enriched radiation remained comparatively short (Figure 1, A) and reached just 79% and 68% of control stem length, respectively (Figure 1, B; $P < 0.05$; Table 1).

The UV-mediated decrease in elongation growth was not limited to plant height. A similar impediment of elongation could be observed for petioles. The typical petiole length for a control plant ranged between 1.5 and 11.9 cm for the seventh and the third leaf, respectively.

However, petioles of plants exposed to UV-A- or UV-B-enriched radiation remained considerably shorter (Figure 2). The relative effect of UV-A-enriched radiation was more-or-less constant across the range from older to younger leaves, not exceeding more than 17% inhibition. The decrease in petiole length was significant ($P < 0.05$) in UV-A-exposed plants for the first, second, and third petiole only (Table 1). In contrast, the effects of UV-B-enriched radiation were particularly pronounced for the youngest leaves (fifth, sixth, and seventh petiole), with petiole length decreasing by more than 40% compared with control plants. This UV-B-induced decrease was significant for the first–seventh petioles (Table 1). Also, progressive decreases in petiole length under UV-B-

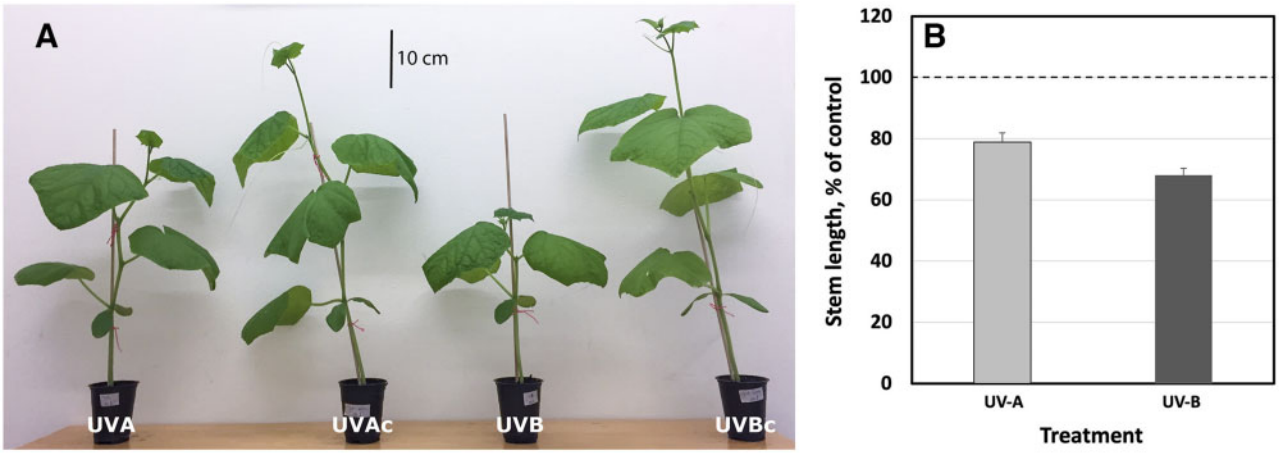

Figure 1 Plant size of cucumber plants grown under different light conditions. A, Example of phenotype of plants exposed to UV-A- and UV-B-enriched light and their corresponding non-exposed controls (UVAc and UVBc, respectively). B, The relative change in stem length of cucumber plants grown under UV-A-enriched (light gray) or UV-B-enriched (dark gray) light, respectively, compared with the corresponding controls. The data represent mean values with $n = 18$ for all treatments and controls ± estimated 95% confidence interval (whiskers) of the ratio obtained from the approximated standard deviation which in turn was obtained by Taylor linearization (Taylor, 1997). The pairwise comparisons UV-A:control, UV-B:control, and UV-A:UV-B were all significant ($P < 0.05$; see Table 1).

Table 1 Significant differences between means of measured variables with regard to treatment and where "*x*" denotes $P < 0.05$

Plant part	Parameter	UV-A:control	UV-B:control	UV-A:UV-B	Figure number
Stem	Length	x	x	x	1
First petiole	Length	x	x	x	2
Second petiole	Length	x	x		2
Third petiole	Length	x	x	x	2
Fourth petiole	Length		x	x	2
Fifth petiole	Length		x	x	2
Sixth petiole	Length		x	x	2
Seventh petiole	Length		x	x	2
Second true leaf	Area	x	x		3A
Third true leaf	Area		x	x	3A
Fourth true leaf	Area		x	x	3A
Total leaf	Area	x	x	x	3B
Second true leaf	Dry mass		x	x	3C
Third true leaf	Dry mass	x	x	x	3C
Fourth true leaf	Dry mass	x	x	x	3C
Second true leaf	SLA	x	x	x	4A
Third true leaf	SLA	x	x	x	4A
Fourth true leaf	SLA	x		x	4A
Total leaf	SLA	x		x	4B
Total plant	Dry mass	x	x	x	5A
	Shoot/root ratio	x			5B
	LMF	x	x	x	5C

T tests were used for total plant or leaf parameters, whereas paired *T* tests were used for petiole and true leaf parameters comparing developmental effects on same plant individuals. Petioles and leaves are numbered in order of appearance, with higher numbers for younger structures.

enriched radiation were found to be statistically significant when comparing adjoining petioles 1–6 (Table 2), that is a larger decrease the younger the tissue. However, there was no statistically significant difference in the extent of the decrease when comparing the small, developing petioles 6 and 7.

LA was also affected by UV light. Generally, only small changes in LA were obtained following treatment with UV-A-enriched light (Figure 3, A and B). Yet, exposure to UV-B-enriched light led to considerable decreases in LA. The UV-B-induced alteration was more pronounced for younger leaves, as is shown in Figure 3, A for true leaves 2–4 (15%, 24%, and 35% smaller leaves, respectively). For the UV-B treatment, these changes were all statistically significant ($P < 0.05$), whereas for UV-A only the 10% decrease in LA (Figure 3, A) of true leaf No. 1 was statistically significant

(Table 1). In addition, the progressive decrease in true LA under UV-B-enriched radiation was statistically significant for true leaf 2 compared with leaf 3, and leaf 3 compared with leaf 4 ($P < 0.001$; Table 2), confirming a larger decrease the younger the tissue. At the whole plant level, this resulted in a statistically significant decrease in LA by 5% for plants exposed to UV-A-enriched light and by 28% for plants grown under UV-B-enriched light (Figure 3, B). In parallel, UV-B exposure caused a statistically significant decrease in leaf dry weight for true leaves 2–4 (Figure 3, C and Table 1), while UV-A exposure caused a small increase.

The observed decrease in LA, together with a slightly larger decrease in leaf mass in plants exposed to UV-B-enriched light (Figure 3, A versus C), results in a statistically significant increase in specific LA (SLA) in the second and third leaves (Figure 4, A and Table 1). The older the leaves, the larger the increase in SLA. A similar trend was also seen in the total plant SLA (Figure 4, B) which, however, was not statistically significant. In contrast, a clear and statistically significant negative effect of UV-A-enriched light on second, third, and fourth leaf SLA as well as on total plant SLA is discernible, with total SLA decreasing by as much as 18% compared with control leaves (Figure 4, B and Table 1). There was a statistically significant difference in SLA between plants exposed to UV-A- and UV-B-enriched light in all cases (Figure 4, A and B and Table 1).

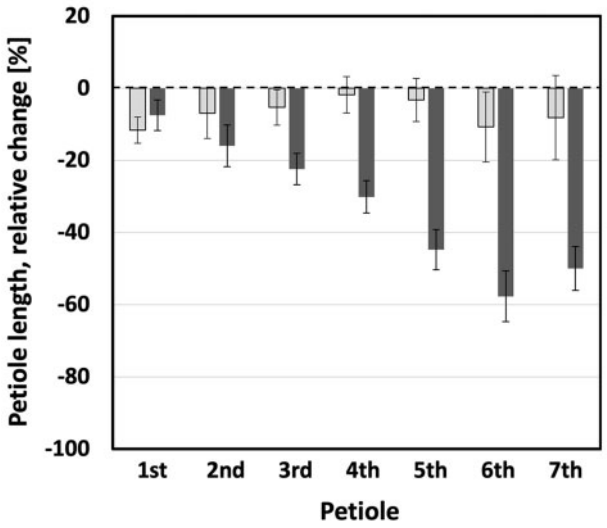

Figure 2 Petiole lengths in cucumber plants grown under different light conditions. The relative decrease of the lengths of the first–seventh petioles of cucumber plants when grown 14 days under UV-A-enriched (light gray) or UV-B-enriched light (dark gray), respectively, compared with the corresponding controls. The data represent mean values with $n = 18$ for all treatments and $n = 36$ for controls ± 95% confidence interval obtained using the approximated standard deviation which was obtained by Taylor linearization (Taylor, 1997). The significant differences ($P < 0.05$) of the pairwise comparisons UV-A:control, UV-B:control, and UV-A:UV-B are shown in Table 1.

To explore whether the more compact architecture of plants exposed to UV-A- or UV-B-enriched light was related to an overall decrease in growth, both biomass and photosynthetic activity were measured. The dry weight of control plants ranged between 3.8 and 4.6 g (average 4.2 g) after 28 days of growth. Overall, UV-A-enriched radiation significantly stimulated plant biomass production by 14% relative to the control (Figure 5, A and Table 1). In contrast, UV-B-enriched radiation had a clear negative impact on biomass accumulation. The statistically significant decrease in biomass caused by UV-B was 28% (Figure 5, A and Table 1). UV-A also impacted on the shoot-to-root ratio, resulting in a 22% decrease (Figure 5, B and Table 1) due to the relatively high root biomass in plants exposed to UV-A-enriched light. No such effect was seen in plants exposed to UV-B-enriched light. A small but statistically significant increase in the leaf weight fraction, relative to the controls (Figure 5, C and Table 1), was induced by both UV-A and UV-B.

To understand the underlying cause of the observed alterations in plant morphology, we explored whether UV-exposed plants exhibited disrupted metabolism as a response to stress. Photosynthetic activities were monitored using chlorophyll fluorometry throughout the experiment for all treatments. The initial measurement of F_v/F_m on the four measuring days did not differ between treatment nor day and was 0.792 ± 0.012 (Supplemental Figure S1). Thus, the photosynthetic response did not change over time (Supplemental Figure S2) and just data from day 15, the first day after the end of the UV enrichment, are presented (Figure 6). The measurements were done on the youngest well-developed leaf and followed by exposure to actinic light at low (302 μmol m^{-2} s^{-1}) and high (1860 μmol m^{-2} s^{-1}) PAR. The lower PAR corresponded to a level in the range that the plants experienced during most of the day in the

Table 2 Pairwise comparisons for statistical significance (paired *t* test) of petiole length and true LA in plants exposed to UV-B-enriched light and where ** is $P < 0.01$; *** is $P < 0.005$; and **** is $P < 0.001$

Treatment	Parameter	Plant part 1	Plant part 2	Level of significance	Figure number
UV-B-enriched	Petiole length	First petiole	Second petiole	***	2
		Second petiole	Third petiole	**	2
		Third petiole	Fourth petiole	****	2
		Fourth petiole	Fifth petiole	****	2
		Fifth petiole	Sixth petiole	****	2
		Sixth petiole	Seventh petiole	****	2
UV-B-enriched	True LA	Second true leaf	Third true leaf	****	3A
		Third true leaf	Fourth true leaf	****	3A

Petioles and leaves are numbered in order of appearance, with higher numbers for younger structures.

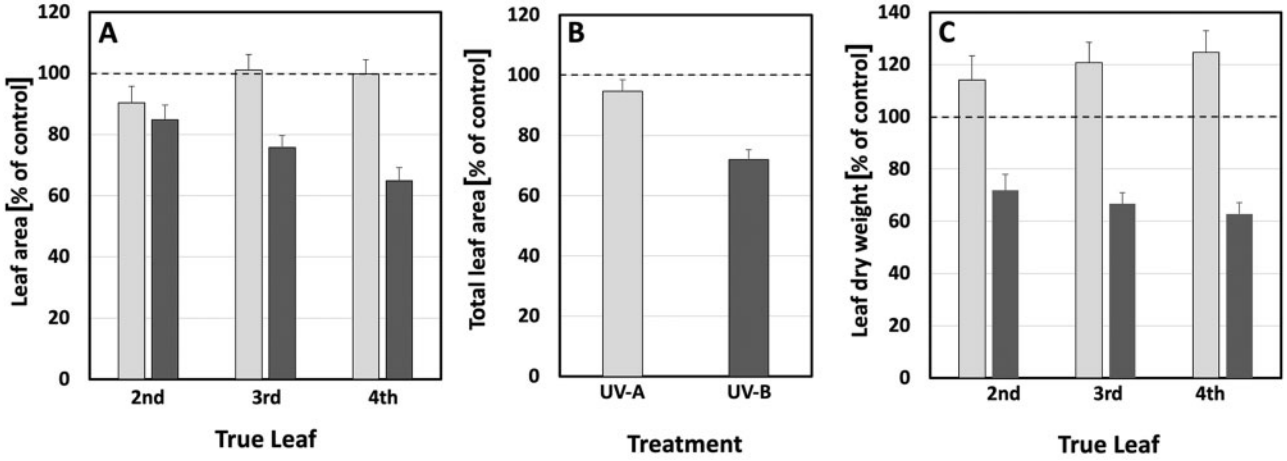

Figure 3 Leaf parameters in cucumber plants grown under different light conditions. A, The relative change in LA of true leaves 2–4. B, Total LA. C, Dry weight of true leaves 2–4, compared with the corresponding controls when grown under UV-A- or UV-B-enriched light, respectively. The data represent mean values with $n = 18$ for all treatments and $n = 36$ for controls ± the estimated 95% confidence interval (whiskers) of the ratio obtained using the approximated standard deviation which was obtained by Taylor linearization (Taylor, 1997). The significant differences ($P < 0.05$) of the pairwise comparisons UV-A:control, UV-B:control, and UV-A:UV-B are shown in Table 1.

greenhouse, while the high level corresponded to light saturation, where potential differences in light acclimation are most clearly shown. Despite the exposed position of the youngest fully developed leaf and exposure to the treatments for the entirety of its development, the operation efficiency of PSII (F_q'/F_m'; Figure 6, A) and fraction of open PSII (q_L; Figure 6, B) were both unaffected by UV treatments. The only treatment effect was a small but significant increase in heat dissipation through NPQ (Figure 6, C) in cucumbers grown in UV-A-enrichment. This was not a big enough increase to affect F_q'/F_m' and q_L, indicating that photosynthesis was not affected by the UV enrichment.

In parallel to measurements of the photosynthetic activity, chlorophyll content was measured using a Dualex. For the duration of the experiment, the first true leaf slowly accumulated more chlorophyll per unit of LA (Figure 7, A). Treatment with UV-A- or UV-B-enriched radiation had no impact on this process. Likewise, in the youngest well-developed leaf, measured on day 15, one day after the end of UV treatment, there was no statistically significant effect of UV-A or UV-B on chlorophyll content (Figure 7, B).

A key component of plant UV protection is the accumulation of flavonols and related compounds. Here, we show a complex induction curve using two independent approaches that both peaked 5 days after commencement of UV treatment. LAEFC measurements (using the Dualex instrument) revealed that UV-B-enriched, and to a lesser extent UV-A-enriched, radiation-induced accumulation of flavonols in the second true leaf (Figure 8, A) compared with control plants. These changes were statistically significant for days 3, 5, and 10 of exposure (Supplemental Table S1). The same pattern can be observed in TUAP, reflecting the total leaf content of flavonoids. Here, the absorbance at 330 nm of methanolic extracts of leaf discs from UV-B exposed plants increased significantly on days 3, 5, and 10 compared with control plants. To a lesser extent this was also the case for plants exposed to UV-A-enriched light (Figure 8, B), showing significantly higher TUAP than control plants on days 3 and 5 of exposure (Supplemental Table S1).

To ascertain to what extent the two analytical methods describe the same physiological process within the plant leaf (i.e. that the two different pools of flavonoids measured by these techniques were directly proportional to each other), two models were adapted to describe the relationship between the methods (see also Supplemental Figure S3). The model best describing the dependence between the results of the LAEFC and TUAP methods considered treatment (UV-A- or UV-B-enriched, or control) and leaf age:

$$\hat{y} = 0.42 + 0.044X - 0.0065X3. \quad (1)$$

A small influence of leaf age ($X3$) was found. R^2 of this fit was 0.84. The residual plots show a random pattern on both sides of 0 (Supplemental Figure S4, A and B), thus justifying the model assumptions that leaf age is also a determinant of the relationship between LAEFC and TUAP. Furthermore, and provided that the linear relationship is valid also for $x <$ the observed values, a zero level in the TUAP parameter (i.e. at the intercept of the axis of the LAEFC parameter) corresponded to a Dualex index of 0.42 in Equation 1, indicating the presence of flavonols in the epidermal cells when the flavonoid level in the bulk of the leaf is negligible.

Linked to the increase in flavonols, a significant increase in total antioxidant capacity (TAC) can be seen in leaves exposed for 3 or 5 days to UV-B-enriched light. To a small extent, leaves exposed to UV-A-enriched light also significantly increased their TAC (Figure 8, C and Supplemental Table S1). Interestingly, whereas both the LAEFC and TUAP parameters on day 14 returned to a level similar to the one

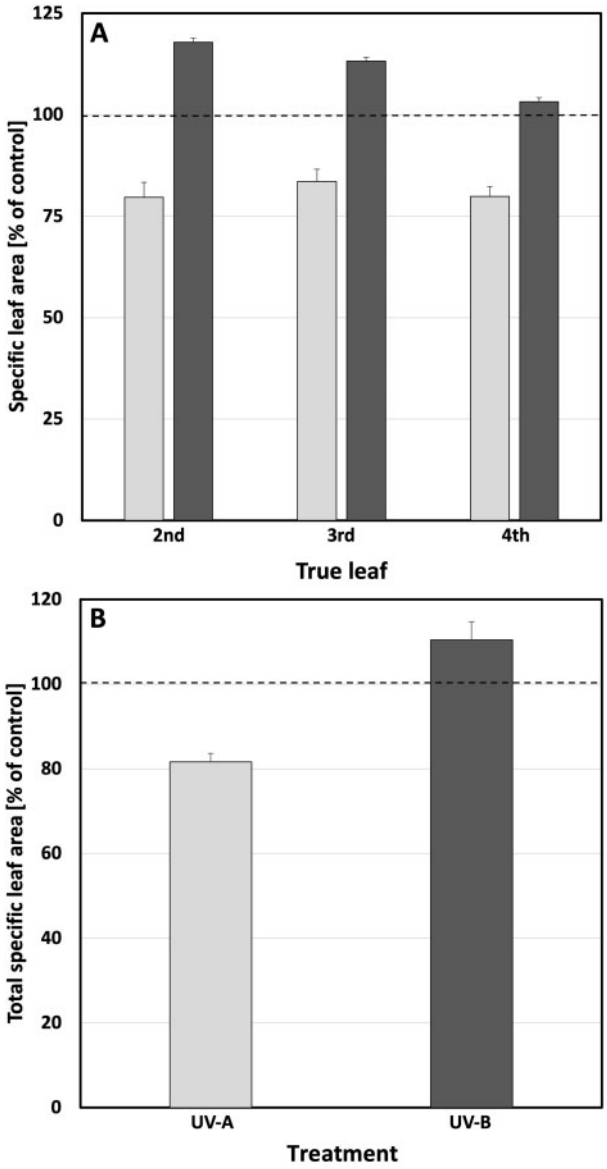

Figure 4 SLA in cucumber plants grown under different light conditions. A, The relative change in SLA (cm^2 mg^{-1}) of true leaves 2–4. B, Total SLA compared with the corresponding controls when grown under UV-A-enriched (light gray) or UV-B-enriched (dark gray) light, respectively. The ratios are based on the mean values with $n = 18$ for all treatments and $n = 36$ controls ± estimated 95% confidence interval (whiskers) obtained using the approximated standard deviation which was obtained by Taylor linearization (Taylor, 1997). The significant differences in SLA ($P < 0.05$) of the pairwise comparisons UV-A:control, UV-B:control, and UV-A:UV-B, are shown in Table 1.

before onset of UV exposure, or slightly below, the TAC parameter decreased significantly to approximately 50% of the initial value, independently of whether the plants had experienced any of the UV exposures or were controls.

To more accurately examine this biphasic nature of the TAC measurements, we studied the dependence between this assay and the two other methods applied in this study (LAEFC and TUAP). To describe the dependence between the TAC and the LAEFC assays, we assumed two simple linear relationships, without taking into account the type of treatment (UV-A- or UV-B-enriched), but dividing up the samples in those from younger leaves ($\leqslant 5$ days of exposure time, i.e. $\leqslant 19$ days after sowing) and those from older leaves ($\geqslant 10$ days of exposure time, i.e. $\geqslant 24$ days after sowing). In this case, the differences of the linear relationships between the TAC and LAEFC assays became apparent, as is shown in Figure 9, A. The model for the linear dependence with regard to young leaves was found to be:

$$\hat{y} = 0.143 + 0.1276X, \quad (2)$$

whereas for the linear dependence with regard to older leaves, the equation was

$$\hat{y} = 0.124 + 0.2068X. \quad (3)$$

R^2 for the fits of data points to the two assumed linear relationships was 0.72 and 0.83, respectively. The intercept at zero TAC level was similar for both linearizations with a LAEFC value of approximately 0.13 (Eqs 2 and 3), indicating a low level of leaf epidermal flavonols that are not active as antioxidants.

Finally, we scrutinized the linear dependence between the TUAP (Figure 8, B) and the TAC methods (Figure 8, C), using the same model as applied above. In Figure 9, B, we again assumed two simple linear relationships, without taking into account the type of treatment (UV-A- or UV-B-enriched), but dividing up the samples in those for younger leaves ($\leqslant 5$ days of exposure time, i.e. $\leqslant 19$ days after sowing) and those from older leaves ($\geqslant 10$ days of exposure time, i.e. $\geqslant 24$ days after sowing). Two linear relationships between the TAC and TUAP data were estimated and the equation with regard to younger tissue was found to be

$$\hat{y} = 2.37 + 0.29X. \quad (4)$$

In this case, the equation explained variation in data with a factor R^2 of 0.91. For older tissue, the equation became

$$\hat{y} = 0.39 + 0.40X. \quad (5)$$

R^2 was even higher (0.98) for the older leaves and the difference between the intercepts at 0 absorbance for TUAP differed approximately six-fold (0.39–2.37).

To further understand the link between UV exposure and induced changes in plant morphology, accumulation of CPD dimers was measured in leaves of plants exposed to UV-A- or UV-B-enriched light and in control plants to see whether induced CPDs were associated with the smaller cucumber phenotype. Overall, the number of CPDs was low, and, with the exception of day 14, variability was limited. There were no statistically significant effects of UV-A or UV-B on CPD accumulation (Figure 10).

Finally, to explore whether changes in key plant hormones are associated with observed changes in plant morphology, leaf concentrations of abscisic acid (ABA), gibberellins (GA), and the auxins indole acetic acid (IAA) and indole-butyric acid (IBA) were quantified. Statistically significant decreases in ABA, IAA, and IBA were associated with leaf development

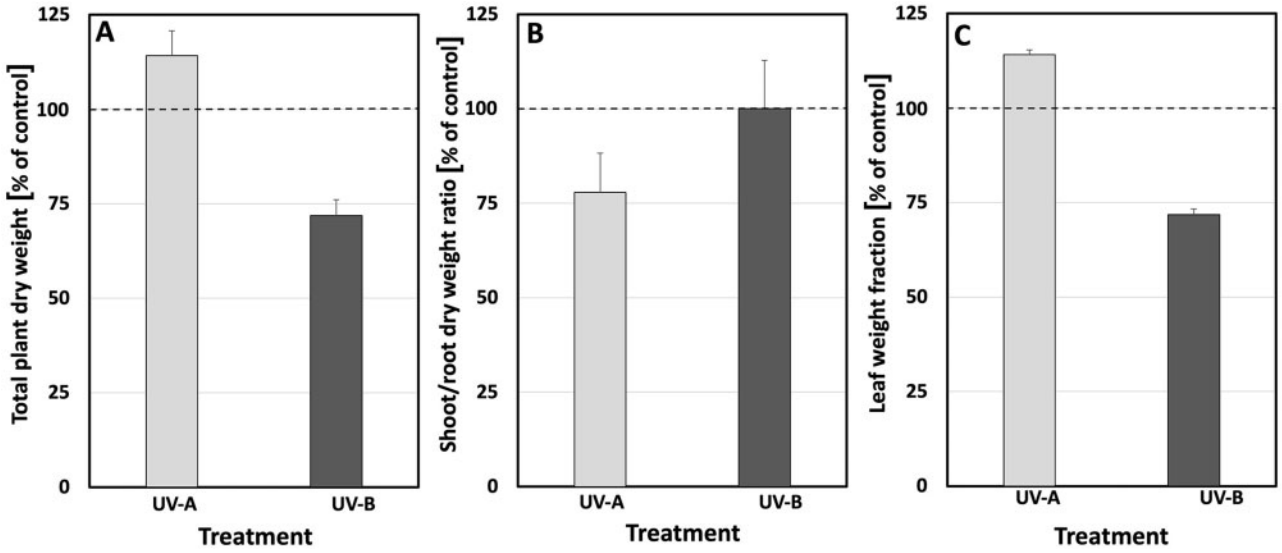

Figure 5 Whole plant parameters in cucumber plants grown under different light conditions. A, The relative change in plant DM. B, Shoot/root DM ratio. C, Leaf weight fraction with the corresponding controls when grown under UV-A-enriched (light gray) or UV-B-enriched (dark gray) light, respectively. The ratios are based on the mean values with $n = 18$ for all treatments and $n = 36$ for controls ± estimated 95% confidence interval (whiskers) obtained using the approximated standard deviation which was obtained by Taylor linearization (Taylor, 1997). The significant differences ($P < 0.05$) of the pairwise comparisons UV-A:control, UV-B:control, and UV-A:UV-B are shown in Table 1.

(Table 3). No statistically significant effects of UV treatment were observed, although small decreases in the GA GA1, GA44, GA6, and GA15 were noted in plants exposed to either UV-A- or UV-B-enriched radiation (Table 3).

Discussion

Cucumber displays a strong morphological response when exposed to supplemental UV

Here, we explored the regulation of plant morphology by white light enriched with either UV-A or UV-B. The data show that enrichment of the spectrum with either UV wavelength results in a stocky cucumber phenotype. These data are in agreement with previous studies that show that cucumber is particularly responsive to UV-exposure (Krizek, 1978; Murali and Teramura, 1986; Ballaré et al., 1991; Adamse and Britz, 1992; Adamse et al., 1994; Krizek et al., 1994, 1997; Takeuchi et al., 1996; Fukuda et al., 2008; Shinkle et al., 2010; Yamasaki et al., 2010, 2014; Qian et al., 2019, 2020). Therefore, we consider cucumber a promising model species for the study of the stocky UV phenotype, a role that will be facilitated by the large leaf surface area which enables measurement of potential hormone gradients within organs. The data presented in this study show that especially elongation is affected by UV-exposure, with noted decreases in stem and petiole length, as well as in LA. These effects were larger in plants that had been grown in the UV-B-enriched than in the UV-A-enriched light environment (Figures 1, 2, and 3, A and B). Interestingly, whereas the petiole lengths and LA in plants treated with UV-A-enriched light were approximately the same independent of tissue age, there was a progressively larger decrease in these parameters the younger the tissue in the presence of UV-B radiation (Figures 2, 3, A and Table 2). Finally, in plants grown under the UV-A-enriched light regimen, a significant reallocation of photosynthate from shoot to root by more than 20% was seen (Figure 5, B). The differences between the effects of UV-A- and UV-B-enriched light on cucumber morphology indicate that there may be different developmental regulatory mechanisms involved in the two cases.

The overall results are thus consistent with earlier descriptions of the UV phenotype, which referred to a more "stocky" architecture (Barnes et al., 1996; Jansen et al., 1998; Robson et al., 2015b). Other aspects of the UV phenotype, such as leaf thickening are also apparent in the current study, and a decrease in SLA was noted in plants exposed to UV-A-enriched radiation. A similar UV-induced stocky phenotype has been observed in a substantial number of plant species (Robson et al., 2015b). Yet, this phenotype remains an enigma, in that major questions remain to be answered with respect to the wavelength specificity of its induction, the underlying mechanism of the response, and the functional importance of the induced architectural response for the plant.

The stocky UV phenotype is not associated with plant stress

Several hypotheses have, over the years, been proposed to explain the mechanism underlying UV-induced changes in plant morphology (Robson et al., 2015b). High UV intensities can drive the development of stress-induced morphogenic responses (SIMRs) as first proposed by Potters et al. (2007). These responses are associated with the disruption of cellular metabolism (distress), resulting in a localized cessation of growth. Therefore, intensities of the UV light used are key and dose-dependent, as well as UV:PAR ratios (Rai et al.,

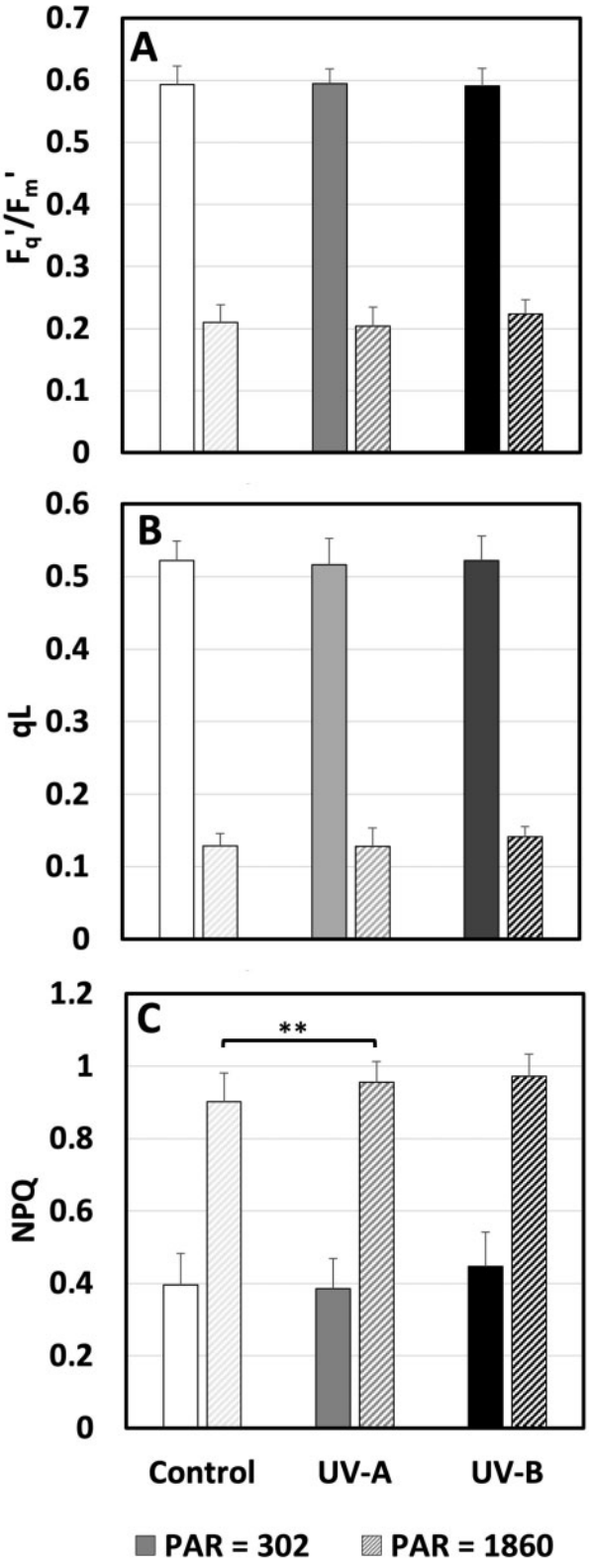

Figure 6 Photosynthetic parameters measured in cucumber plants grown under different light conditions. A, The response of the operation efficiency of PSII (F_q'/F_m'). B, The fraction of open PSII (q_L). C, Heat dissipation measured as NPQ of fluorescence measured on the youngest well-developed leaf under an actinic PAR of 302 or 1860 μmol m^{-2} s^{-1} on day 15 after commencement of UV exposure (last day of UV exposure day 14) to UV-deficient control (white), UV-A-enriched (gray) or UV-B-enriched (black) light. The data represent mean values ± SD with $n = 9$ for UV treatments and $n = 18$ for controls. *T* test was used for statistical analysis. ** were used to represent the significant difference for $P \leqslant 0.01$.

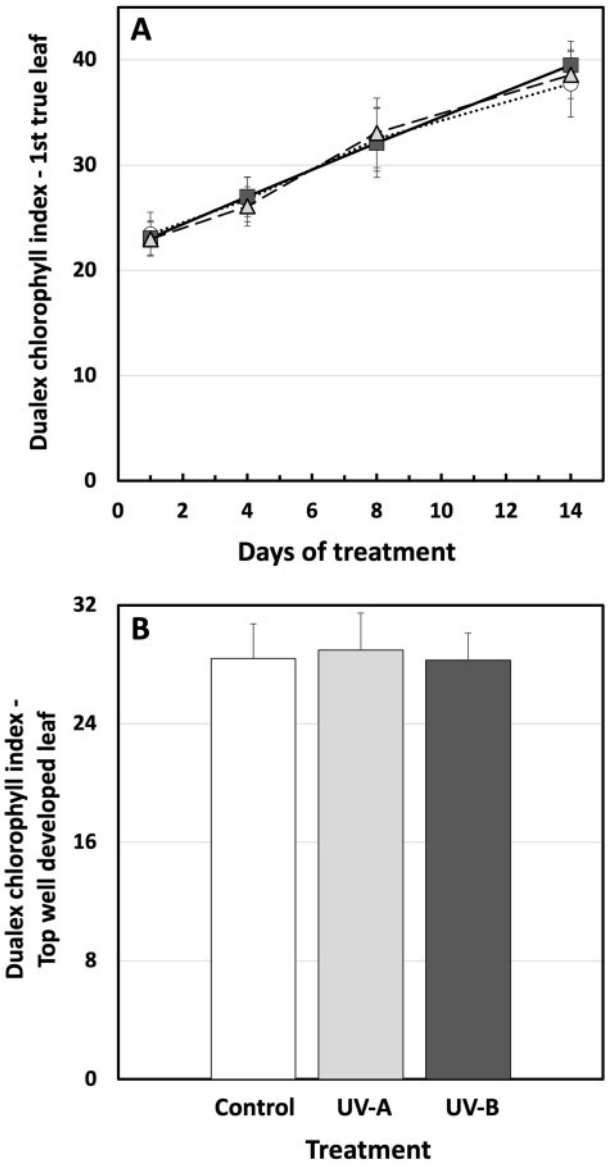

Figure 7 Chlorophyll content in cucumber plants grown under different light conditions. A, The adaxial surface chlorophyll levels expressed as "Dualex chlorophyll index" of the first true leaf of UV-deficient controls (open circles), UV-A-enriched light (gray triangles), and UV-B-enriched light (closed squares) treated plants. B, Adaxial surface chlorophyll levels of the youngest well-developed leaf measured on day 15 after commencement of treatment using UV-A-enriched (light gray) or UV-B-enriched (dark gray) growth light, compared with the corresponding UV-deficient control (white). Sampling was done as in Figure 1. The data represent mean values ± SD, $n = 9$ for the UV-enriched treatments and $n = 18$ for the control. Two-way ANOVA was used to test the effect of exposure time, and treatment on adaxial surface chlorophyll levels of the first true leaf. *T* test was used to test the significant difference of upper surface chlorophyll levels in youngest well-developed leaf between UV-treated and control samples.

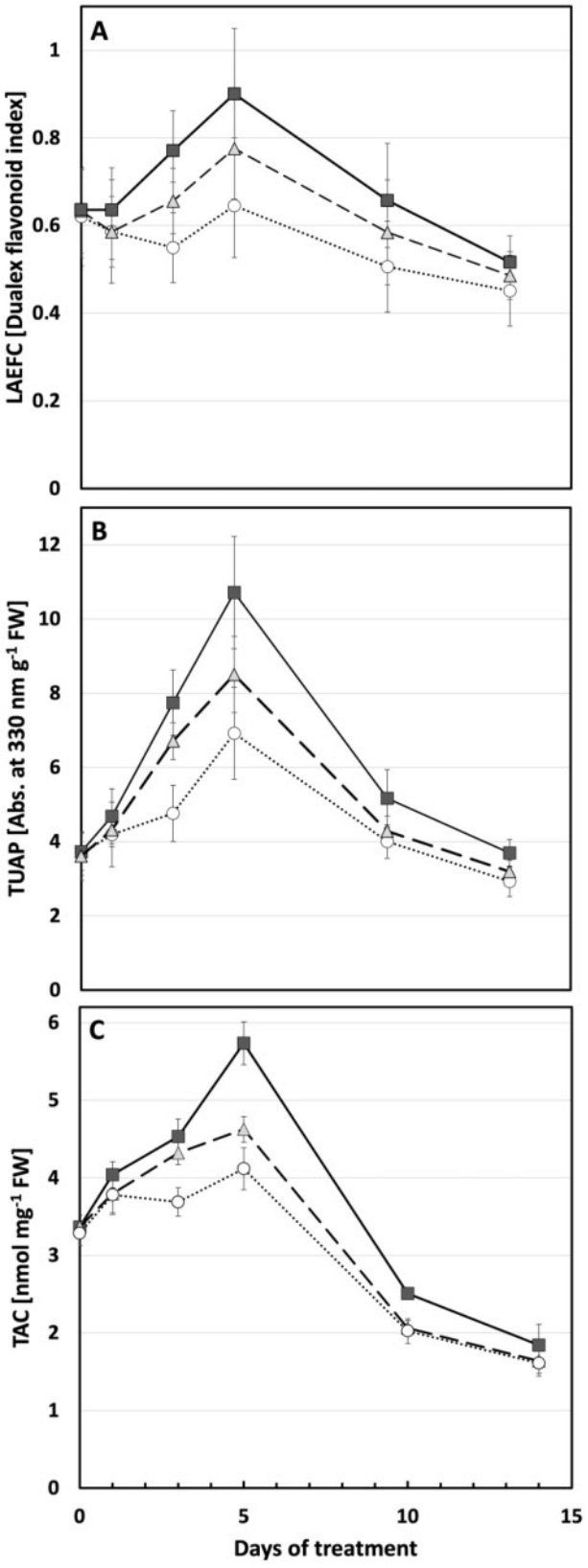

Figure 8 Flavonoid content and antioxidative capacity in cucumber plants grown under different light conditions. A, LAEFC measured with Dualex. B, Total UV-absorbing pigments, TUAP, measured spectrophotometrically at 330 nm per leaf fresh weight. C, TAC measured as nmol Trolox equivalents per mg leaf fresh weight. Measurements were performed on the second true leaf of two-week-old cucumber plants grown under UV-A-enriched (gray triangles) or UV-B-enriched light (closed squares), respectively, and compared with the corresponding controls (open circles). Data represent mean values ± SD with n = 15–18 for the UV-enriched treatments and n = 30–36 for the control treatment in (A); n = 9 for the UV-enriched treatments and n = 18 for the control treatment in (B); n = 3 for the UV-enriched treatments; and n = 6 for the control treatment in (C).

2021). In fact, UV dose–responses remain largely unknown, but those studies that have compared effects of multiple doses on morphological parameters, suggest a complex response curve (Brodfuhrer, 1955; Van de Staaij et al., 1997; Qaderi et al., 2008). A key target for future research is determining the dose that causes the transition from physiological regulation of morphology to SIMR, a transition that is of interest from both a scientific and a horticultural perspective. The SIMR phenotype is characterized by decreased elongation growth, which can result in a stockier phenotype, as described in the current study. However, in the current study, there is no evidence for disruptive stress. There was a small increase in NPQ in plants grown under UV-A-enriched light but no change was found in neither maximum photochemical efficiency, redox state of PSII, nor the operation efficiency of PSII in any of the UV treatments measured using chlorophyll *a* fluorometry, nor in total chlorophyll content. Furthermore, there is no evidence for an increase in accumulation of damaged DNA in the form of CPD dimers. DNA damage may potentially result in a stocky phenotype as UV-induced dimerization of DNA can impair DNA replication, and hence impede cell cycle progression, particularly by slowing the G1-to-S phase (Jiang et al., 2011). Indeed, several earlier reports refer to UV-mediated impairment of cell division (Dickson and Caldwell, 1978; Wargent et al., 2009). Others (Lake et al., 2009) refer to larger cells in UV-exposed plants which can be explained by endoreduplication, resulting in fewer, but bigger cells (Radziejwoski et al., 2011). Plants showing symptoms of UV stress would often have between 50 and 800 CPDs/Mb (Kang et al., 1998; Kalbin et al., 2001; Pescheck et al., 2014). Yet, in the current study, levels of CPDs/Mb were one to two orders of magnitude less, indicating efficient repair of damaged DNA. Therefore, the observed stocky phenotype is not associated with accumulated DNA damage. The data on the ABA content also are consistent with non-stress conditions. Furthermore, the data show increases in total antioxidant activity (TAC) and flavonol concentrations in leaf adaxial epidermis (LAEFC) and the entire leaf (TUAP). Taken together, these data reveal successful UV acclimation. Thus, healthy plants display the stocky UV phenotype, implying that the strong morphological response observed in UV-exposed cucumber seedlings is a regulatory adjustment that is part of the UV acclimation processes involving UV-A and/or UV-B photoreceptors.

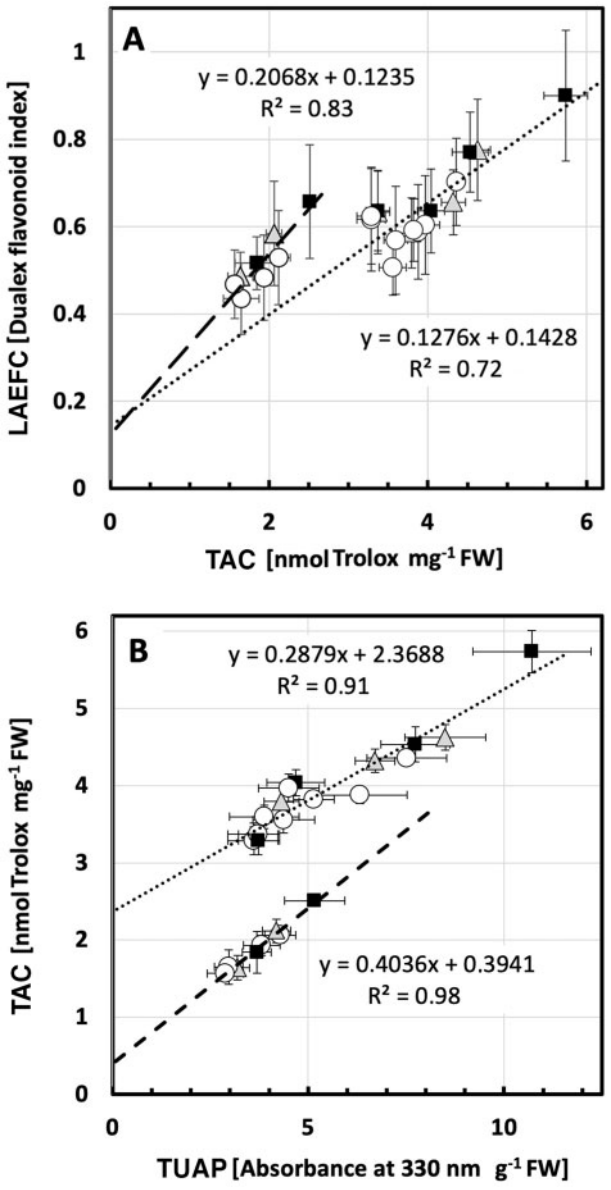

Figure 9 Correlation between TAC and flavonoid-associated parameters in cucumber plants grown under different light conditions. A, The biphasic relationship between TAC and LAEFC (assumed in Eqs 2 and 3) in UV-deficient controls (open circles), plants grown in either UV-A-enriched light (gray triangles) or UV-B-enriched light (closed squares). The dotted line corresponds to younger leaves (Eq. 2), whereas the dashed line corresponds to older leaves (Eq. 3). B, The biphasic relationship between TAC and TUAP (same symbols as in A), assumed in Equations 4 and 5. The dotted line corresponds to younger leaves (Eq. 2), whereas the dashed line corresponds to older leaves (Eq. 3). The data represent mean values ± SD. N = 15–18 for LAEFC UV-enriched treatments and 30–36 for control treatments; n = 3 for TAC UV-enriched treatments and 6 for control treatments; n = 9 for TUAP UV-enriched treatments and 18 for control treatments.

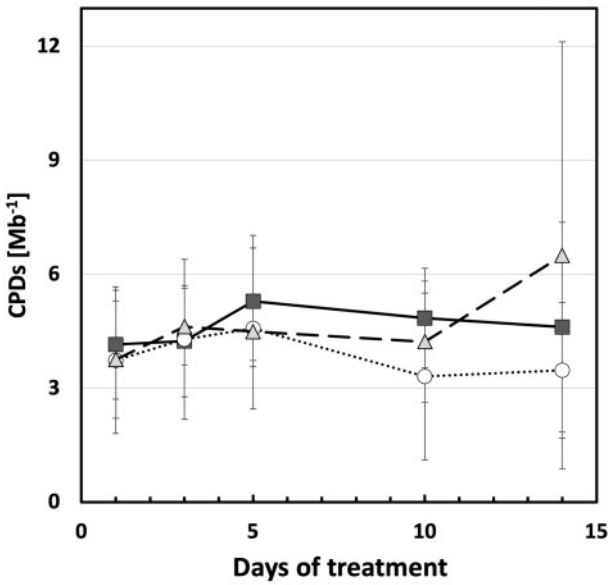

Figure 10 Cyclobutane pyrimidine dimer content in cucumber plants grown under different light conditions. Cyclobutane pyrimidine dimers per mega base (CPDs Mb^{-1}) of the second true leaf during the UV treatments compared with the corresponding controls (open circles) when grown under UV-A-enriched (gray triangles) or UV-B-enriched (closed squares) light, respectively. The data represent mean values ± SD with n = 9 for the UV-enriched treatments and n = 18 for the control treatment. Two-way ANOVA was used to test the effect of exposure time and treatment.

UV acclimation is accompanied by a decrease in biomass accumulation

Notwithstanding the apparent lack of plant stress under either UV-A- or UV-B-enriched light, a substantial decrease in produced total biomass was noted for plants exposed to UV-B-enriched light. We have interpreted this decrease in biomass production as a secondary consequence of UV acclimation. UV-B-exposed plants with shorter stems (including shorter internodes) and shorter petioles will condense the same number of leaves in a smaller area, hence increasing the likelihood of self-shading which, in turn, may decrease overall PAR capture, and hence photosynthetic productivity (Barnes et al., 1996). Consistently, UV-A had considerably smaller impacts on both stem and petiole length, and this was associated with a lack of impact on biomass production. UV-B-induced decreases in LA will further hamper PAR capture, an effect that is much smaller in plants raised under UV-A-enriched light. These UV-B-mediated decreases in light capture may also be accompanied by the often-reported UV-B-induced stomatal closure (He et al., 2013; Martínez-Lüscher et al., 2013; Tossi et al., 2014), which would similarly decrease photosynthesis in situ, and potentially decrease biomass production. In addition, the measured UV-A-induced decrease in SLA may potentially improve the water use efficiency of plants (Liu and Stützel, 2004), and although water use efficiency has not been measured in this study, several studies have reported UV-induced co-tolerance with drought (reviewed in Barnes et al., 2019).

Impact of UV-A- and UV-B-enriched light on flowering, fruit setting, and final yield

In a previous horticultural study carried out in two different nurseries over 3 years (Qian et al., 2020), it was found that

Table 3 Main plant hormones, including ABA, GA, and the auxins IAA and IBA), present in the second true leaf on day 3, and 5 of UV treatments

Hormone species	UV-A 3 day control	UV-A 3 day exposed	UV-A 5 day control	UV-A 5 day exposed	UV-B 3 day control	UV-B 3 day exposed	UV-B 5 day control	UV-B 5 day exposed	Trend
ABA	85.5 ± 12.3	96.8 ± 9.0	48.3 ± 12.0	67.7 ± 16.0	71.9 ± 14.1	77.7 ± 3.4	54.9 ± 2.6	52.4 ± 13.4	Significant age-induced decrease
GA1	17.0 ± 7.4	9.7 ± 0.8	13.3 ± 1.2	11.7 ± 3.3	11.1 ± 2.6	10.0 ± 2.8	16.6 ± 5.7	11.7 ± 1.5	Trend of UVA/UVB induced decrease
GA44	2268 ± 1447	1123 ± 342	2104 ± 1214	1315 ± 186	1485 ± 312	1099 ± 298	4850 ± 3668	1184 ± 155	Trend of UVA/UVB induced decrease
GA9	468 ± 288	177 ± 55	424 ± 62	360 ± 120	268 ± 131	184 ± 89	832 ± 626	237 ± 57	Trend of UVA/UVB induced decrease
GA15	2367 ± 1403	839 ± 475	1825 ± 1112	1281 ± 713	1579 ± 944	1035 ± 617	4925 ± 3776	1109 ± 427	Trend of UVA/UVB induced decrease
IAA	84.4 ± 33.4	95.4 ± 3.0	60.2 ± 5.0	67.3 ± 6.6	88.4 ± 20.1	89.9 ± 3.7	67.2 ± 6.2	70.1 ± 7.5	Significant age-induced decrease
IBA	1362 ± 387	1242 ± 67	361 ± 139	522 ± 125	1197 ± 142	865 ± 368	531 ± 100	489 ± 193	Significant age-induced decrease
IBA-OH	1141 ± 357	934 ± 53	278 ± 108	427 ± 126	971 ± 133	696 ± 309	450 ± 90	422 ± 188	Significant age-induced decrease

Notes: Plant tissue from one plant in each of three boxes per treatment was pooled together with three separate experiments giving $n = 3$ for both the UV-enriched treatments and the control treatment. The data represent mean values ± SD and are given in pmol (g fresh weight)$^{-1}$. For data of each plant hormone species, *T* test was used to test the significant difference between each treatment. The levels of the following hormone species were under the detection limit: GA3, GA4, GA5, GA8, GA12, GA19, GA20, IAA-OX, IAA-OH, IBA-OX, IBA-OH-C and IBA-OX-C. The levels of the following hormone species did not show any clear trend: GA7, IAA-C and IBA-C.

flowering, fruit setting, and total fruit yield were not influenced by pre-treatment of plants with UV-A-enriched light for 2 weeks. Two weeks pre-treatment with UV-B-enriched light led to an increased number of flowers in flowering nodes primarily in the third year (Supplemental Figure S3), whereas delayed fruit setting by 2 weeks was found in the experiment carried out in the second year but not in the first or the third year. The total yield of cucumber fruits was however not influenced by either UV-A- or UV-B-enriched light, compared with their corresponding controls, in any of the 3 years (Qian et al., 2020). Thus, apart from the fact that the total yield was not influenced by the treatments, flowering and fruit set was more variable in cucumber plants grown under UV-B-enriched conditions.

Regulatory mechanism(s) underlying the stocky UV-induced phenotype

Since the data in this study do not support an association between the stocky UV phenotype and plant stress, one or more different specific regulatory responses should be considered, as argued above, dependent on what part of the UV spectrum is supplementing the PAR. The UV-B photoreceptor UVR8 was discovered in *Arabidopsis thaliana* mutants that did not show UV-B-induced dwarfing of hypocotyls (Hayes et al., 2014). Thus, UVR8 has been strongly associated with control of plant architecture. It should also be noted that, in a recent study by Rai et al. (2020), there was a marked difference in regulation of gene expression between a UVR8-dominated effect at wavelengths below 335–350 nm and a cryptochrome-dominated regulatory mechanism at UV wavelengths above 350 nm. Notwithstanding, the UVR8- and CRY-regulatory mechanisms were interdependently influenced by each other.

Thus, the mechanism underlying the UV-B-induced stocky phenotype may relate to interactions with various cellular signaling pathways, including the phytochrome and cryptochrome pathways. In UV-exposed plants, UVR8 monomers bind CONSTITUTIVELY PHOTOMORPHOGENIC 1 (COP1), and the resulting UVR8-COP1 complexes enter the nucleus and promote UV-B signaling which inhibits auxin biosynthesis, signaling as well as hypocotyl elongation (Hectors et al., 2012). Parallel increases in the expression of the ELONGATED HYPOCOTYL 5 (HY5)/HY5-HOMOLOG (HYH) transcription factor may enhance transcription of polar auxin transport proteins PIN1 and PIN3, as well as several regulators of auxin signaling (Vanhaelewyn et al., 2016). Furthermore, sequestration of COP1 by UVR8 destabilizes PIF5, further interfering with auxin biosynthesis and signaling (Hayes et al., 2014; Vanhaelewyn et al., 2016). Yet, few studies have been able to demonstrate UV-induced changes in auxin levels. Hectors et al. (2012) reported (non-significant) UV-B-induced decreases in auxin levels in Arabidopsis leaves, as well as altered UV-B responses in auxin influx and biosynthesis mutants (Hectors et al., 2012). The current study does not present evidence for significant changes in auxin concentrations either, despite strong morphological responses, but a non-significant trend of decreasing GA concentrations is observed in both UV-A- and UV-B-exposed plants. UVR8 binding to COP1 can, via upregulation of transcription of HY5 and HYH, result in an increase in gibberellin 2-β-dioxygenase 1 (GA2OX1) levels, reducing GA concentrations (Hayes et al., 2014; Vanhaelewyn et al., 2016). The current study shows a trend of decreasing concentrations of GA1, GA44, GA9, and GA15, in both UV-A- and UV-B-exposed plants. Hormonal action may be important in cross-talk between UV light and other environmental factors affecting for instance plant water use efficiency and drought tolerance (Bernhard et al., 2020). However, the data in the current paper are not conclusive with respect to a role for UVR8, auxin, or gibberellic acid in mediating plant UV responses.

In fact, it is debatable whether the observed dwarfing response can simply be explained as UVR8 mediated, given that responses are induced by both UV-B and UV-A radiation, albeit with partly different outcomes (progressive decreases in petiole lengths and LA in plants grown in UV-B-enriched light; alteration in carbon allocation from shoots toward roots in UV-A-enriched light). Therefore, although the UVR8 action spectrum remains to be fully characterized in detail, particularly with respect to potential interactive responses to UV-A wavelengths, recent evidence suggests antagonistic effects whereby responsivity to UV-B is modulated by UV-A wavelengths and vice versa (Morales et al., 2013; Rai et al., 2020). Thus, although a UVR8-mediated mechanism appears to be the most likely candidate to explain observed decreases in both organ elongation and GA concentration in UV-B-exposed plants, major questions remain to be addressed concerning the regulation of the stocky phenotype under natural, solar light conditions where there is considerable scope for interactions between multiple wavelength bands, photoreceptors, and signaling pathways. In fact, brassinosteroids may also play a role in UV-regulation of gene expression (Sävenstrand et al., 2004) and development (Liang et al., 2018), a role which was further strengthened by the discovery of interaction of UVR8 with molecular regulators of brassinosteroids.

Regulation of cucumber phenylpropanoid genes

The regulation of all 12 different cucumber phenylalanine ammonia lyase (*CsPAL*) genes, all three cinnamate 4-hydroxylase (*CsC4H*) genes, and all three chalcone synthase (*CsCHS*) genes, as the result of exposure to UV-A- and UV-B-enriched light, has previously been reported (Qian et al., 2019). The proteins encoded by these genes encode the PAL, C4H, and CHS isoenzymes of the phenylpropanoid pathway that are all involved in the synthesis of flavonoids, including flavonols. Some of the genes were up-regulated by UV-A and others by UV-B. In particular, three of the latter genes (*CsPAL4*, *CsPAL10*, and *CsCHS2*) were up-regulated at least 30-fold by UV-B exposure. These three genes had in common an enrichment of upstream cis-acting elements (MREs, ACEs, and G-boxes) that may be of importance for amplification of expression of flavonoid biosynthesis genes under UV-B-containing light (Qian et al., 2019). Therefore, it is obvious that there are distinct regulatory effects by UV-B and UV-A on genes of importance for UV tolerance in cucumber.

Relationships between flavonoid content and antioxidant capacity

Protection against UV light was measured in three different ways reflecting the notion that UV-B-induced flavonoidal compounds have both an antioxidative effect and a function as UV-absorbing compounds (Agati et al., 2012; Hideg and Strid, 2017). For estimation of leaf adaxial epidermal flavonol content (LAEFC), the Dualex method was used, for TUAP acidic methanol extraction and spectrophotometric detection at 330 nm was employed, and total anti-oxidative activity (TAC) was assayed using the Trolox method. Comparisons between LAEFC and TUAP measurements have been made previously (Barthod et al., 2007), and in line with published results the intercept of the plot of LAEFC versus TUAP measurements (Supplemental Figure S1) is inferring higher flavonol content in the epidermal cell layers compared with the average in the total foliar biomass.

The data of this paper show an increased flavonoid level in leaves for up to 5 days after all three treatments (no UV control, UV-A-, or UV-B-enriched light). Thereafter, the flavonoid content declined (Figure 8, A and B). The dependence of the flavonoidal levels (LAEFC and TUAP), with a peak at Day 5 is likely to be due to leaf developmental processes. TAC also peaked on day 5 (Figure 8, C). That the peaks in all three parameters at Day 5 could be related to particular weather conditions seem highly unlikely given that all experiments were independently replicated three times during different weeks between February and June. For TUAP, readings after 14 days of UV exposure were similar to those measured at the onset of the experiment (day 0). For the LAEFC, the readout on day 14 returned to levels slightly lower than at the outset, whereas for TAC the antioxidant capacity decreased between day 0 and day 14 by about 50%, independently of whether the plants had experienced any UV exposures or were controls. Thus, as these trends were observed in both control and in UV-treated plants, a developmental process would be the likely cause. To improve understanding of developmental processes as well as the relationships between the three different parameters, further regression analyses were performed.

The shape of the TAC curve of antioxidant capacity when compared LAEFC or TUAP results indicate that the TAC parameter reflects two different physiological means of antioxidative activity, one being flavonoids and the second being another type of ROS scavenging of enzymatic or non-enzymatic nature, and which shows an age-dependent decrease by half through days 10–14. When estimating the linear dependence of the TAC and LAEFC experiments, we found that the intercept at a zero TAC level was similar for the two leaf-age-dependent linearizations used (Eqs 2 and 3), with a LAEFC flavonol index of approximately 0.13 (Figure 9, A), which indicates the presence of some flavonoidal compounds that lack antioxidant capacity, for example monohydroxylated species (Agati et al., 2012). Differences in the antioxidant capacity of different flavonol species have been extensively demonstrated (Csepregi et al., 2016). For example, some flavones, such as apigenin, have particularly low ferric ion reducing antioxidant power (Csepregi et al., 2016). Also, it should be considered that Trolox may not be a perfect proxy for antioxidant activity in general (Csepregi et al., 2016).

The difference in the slope of the two linear relationships in Supplemental Figure 9, A and the different shapes of the curves in Figure 8, A and B, indicate that, as the leaf tissue aged, the pool of leaf epidermal flavonols had lost its antioxidative capacity, either by accumulation of more oxidized

forms of this type of compound, because of increased *O*-glycosylation, or due to another yet to be identified mechanism. The OH group on the 3-position on the A-ring of the flavonoid backbone is commonly glycosylated, which decreases antioxidant activity. Developmental changes in flavonol profiles have also previously been shown in for instance white mustard (*Sinapis alba*; Reifenrath and Müller, 2007) and grapevine (*Vitis vinifera*; Bouderias et al., 2020). Also, a study by Morgenstern et al. (2014) shows that the ratio of quercetin to kaempferol in buckthorn (*Hippophaë rhamnoides*) shows a strong developmental trend, rising from just over 100 at the beginning of the season, to over 400 by mid-summer, and this effect is paralleled by a drop in gallic acid and rutin levels (Morgenstern et al., 2014). Given the different antioxidant activities of different flavonols, this may underpin a change in antioxidant capacity.

In our study, the loss of anti-oxidative defense (i.e. TAC) was independent of whether the plants had been kept under control conditions or under supplementary UV-A- or UV-B-enriched light. Thus, this seems to be a true effect of leaf age. In old leaves, flavonoids constitute the bulk of the antioxidant capacity (intercept close to 0 in Figure 9, B), whereas in younger tissue half of the oxidant capacity (comparison of the curves in Figure 8, B and C and considering the intercept at 2.37 in Figure 9, B) is contributed by antioxidative systems other than flavonoids, be it enzymatic or non-enzymatic, that do not absorb light at 330 nm in methanol under acidic conditions. Leaf age-dependent changes in TAC have previously been shown in greenhouse-grown grapevine leaves (Majer and Hideg, 2012), using a several-fold higher biologically effective UV-B dose than we did. Four days of exposure led to a large increase in TAC in young leaves, similar to what we found in cucumber. However, in old leaves, 4 days of UV exposure led to decreased TAC. Clearly, there are strong interactions between UV acclimation and developmental processes that govern as disparate physiological parameters in plants as stem and petiole stretching, leaf expansion, flavonoid content, and TAC.

Conclusion

In this paper, we show that cucumber grown in UV-A- or UV-B-enriched light led to a stockier phenotype compared with non-UV-irradiated control plants. In plants grown in UV-A-enriched light, the decreases in stem and petiole lengths were similar independent of tissue age whereas in plants grown in UV-B-enriched light stems and petioles were progressively shorter the younger the tissue. In addition, plants grown under UV-A-enriched light significantly reallocated photosynthates from shoot to root, had thicker leaves, and decreased SLA. This infers different morphological plant regulatory mechanisms under UV-A and UV-B radiation, especially since there was no evidence of stress in any of the UV-exposed plants, as judged by the absence of effects on photosynthetic parameters, cyclobutane pyrimidine dimer levels, or ABA content. The total leaf antioxidant activity and UV-dependent accumulation patterns of flavonoidal compounds and leaf-age-dependent variation in these parameters also indicated successful acclimation of the plants to the two UV light regimens. Therefore, we conclude that the stocky UV phenotype developed in healthy plants, which in turn implies a strong regulatory adjustment and morphological response as part of a successful UV acclimation processes involving UV-A and/or UV-B photoreceptors.

Materials and methods

Plant material, growth conditions, and treatment conditions

Cucumber seeds (*C. sativus* L. cv "Hi Jack") were sown one seed per 0.25 L pot in 14-7-15 NPK fortified peat (SE Horto AB, Hammenhög, Sweden), as described previously (Qian et al., 2019, 2020). Seedlings were grown in a greenhouse under natural daylight from the roof which was supplemented with 150–200 μmol m^{-2} s^{-1} PAR as measured 20 cm above the table using Vialox NAV-T Super 4Y high-pressure sodium lamps (Osram, Johanneshov, Sweden) for 16 h per day centered around solar noon, and only turned off when the natural irradiance reached 900 μmol m^{-2} s^{-1}. The day/night temperature was 25°C/20°C and the relative humidity was set to 80%. Watering was done by adding water to the tray underneath the pots when the tray itself was completely dry. As soon as the cucumber seedlings had fully developed cotyledons, watering was commenced using a full nutrient solution (Svegro AB, Ekerö, Sweden).

Fourteen days after sowing, when the first true leaf of the cucumber seedlings was approximately 5 cm in diameter (about one-third of the diameter of a fully developed first true leaf), UV exposure commenced. The plants were then given either supplementary UV-A-enriched or UV-B-enriched irradiation for 4 h per day (centered around solar noon) in addition to the PAR described above. Controls were simultaneously exposed to PAR only (see below) in the same chamber as the corresponding UV-treated plants. The UV-A and UV-B exposures were carried out in separate greenhouse chambers and the treatments were alternated between the chambers when repeating the experiment (cf., Qian et al., 2019, 2020, for details).

Open top, front, and backside boxes (OTFB boxes), covered with Perspex on the left and right sides, were used for the different UV exposures. Each greenhouse compartment was equipped with up to six boxes, three being used for the UV treatments and three for the corresponding controls. Each OFTB box contained up to 48 plants per replicate. For the UV-A-enriched experiments, fluorescent UVA-340 tubes (Q-Lab, Cleveland, OH, USA) were used for exposure, whereas for the UV-B-enriched experiments, fluorescent Philips TL40/12 UV tubes (Eindhoven, The Netherlands) were employed. For the control OFTB boxes, UV-blocking Perspex was used to cover the top and all sides. For the UV-B-enriched experiment, 0.13-mm cellulose acetate (Nordbergs Tekniska AB, Vallentuna, Sweden) covered the top, front, and backside of the OTFB boxes with the purpose to remove any UV-C radiation emitted by the Philips

TL40/12 tubes. For the UV-A-enriched experiment, the OFTB boxes were similar to the boxes used in the control experiment but without any filtering material on top.

The spectral distribution of the light environments in the different treatments was measured using an OL756 double monochromator spectroradiometer (Optronic Laboratories, Orlando, FL, USA) 20 cm above the table. The details of doses were as described by Qian et al. (2019). Briefly, however, UV-A-enriched radiation contained 3.6 W UV-A m^{-2} and a 45.5 mW m^{-2} plant-weighted UV-B (calculated according to Yu and Björn, 1997), giving a total of plant-weighted UV-B of 0.6 kJ m^{-2} day^{-1} during the daily 4-h exposure. The UV-B-enriched irradiation had 83.4 mW m^{-2} plant-weighted UV-B totaling 1.23 kJ m^{-2} day^{-1} plant-weighted UV-B. This exposure also contained 0.34 W UV-A m^{-2}. The daily irradiation outside in Lund, Sweden, under clear skies on a summer's day is approximately 4.8 kJ m^{-2} day^{-1} of plant-weighted UV-B (Yu and Björn, 1997).

Morphological measurements

Between day 0 and day 14, morphological parameters were measured. A ruler was used to measure the lengths of stems and petioles. The dry matter (DM) of shoots (separated into stems, petioles, and leaves) and roots was measured using a digital balance (accuracy 0.001 g) following oven drying at 70°C for 20 h. The leaf mass fraction (LMF) was calculated as LMF = leaf DM/total shoot DM. The LA was determined from digitized photographs using ImageJ (https://imagej.nih.gov/ij/). As a measure of how much LA a plant builds with a given amount of leaf biomass, the SLA for true leaves 2–4 from the base of the plants, as well as for all leaves combined, was calculated as SLA = LA/leaf DM. For each experiment, six plants per treatment were measured, two from each of the three replicated treatment OTFB boxes and their corresponding controls. In total, three independent experiments were performed.

Chlorophyll fluorescence

Chlorophyll *a* fluorescence was measured with a MINI-PAM (Walz, Effeltrich, Germany) on the first true leaf from the bottom of the stem on days 1, 4, 8, and 14 of UV exposure, as well as on the youngest well-developed leaf (the top leaf which was fully developed, i.e. the diameter reached approximately 15 cm) on day 15 of UV exposure.In dark, the middle portion of attached leaves were fixed in a leaf clip holder (2030-B, Walz) fitted with a halogen lamp (2050-HB, Walz) and a heat absorbing glass filter (Calflex, Optic Balzers, Liechtenstein). The leaves were then dark adapted for 30 min using aluminium foil. F_o and F_m were measured and the maximum photochemical efficiency of photosystem II (PSII) was calculated as $F_v/F_m = (F_m–F_o)/F_m$. Subsequently, the leaf was exposed to actinic PAR of 302 or 1860 µmol m^{-2} s^{-1} for 10 min to achieve steady-state F_s and F_m', measured by 0.6 s saturating pulses. The operation efficiency of PSII (F_q'/F_m'), where $F_q' = F_m'–F_s$, the fraction of open PSII expressed as q_L, and non-photochemical quenching (NPQ) were calculated as reviewed by Murchie and Lawson (2013). For each experiment, three plants per treatment were measured (one from each of the three replicated treatment OTFB boxes with accompanying control boxes) and in total three independent experiments were performed.

Biochemical analysis

Upper surface chlorophyll content in the first true leaf (on days 1, 4, 8, and 14 of UV exposure), and the youngest well-developed leaf on day 15 of UV exposure was measured using a DUALEX (Force-A, Orsay, France), following chlorophyll fluorescence measurements.

LAEFC in the second true leaf (on days 0, 1, 3, 5, 10, and 14 of UV exposure) was measured using a DUALEX (Force-A) with $n = 15–18$ for the UV-enriched treatments and $n = 30–36$ for the control treatment. Additionally, total UV-absorbing pigments (TUAP; mostly flavonoids) were extracted from the second true leaf (on days 0, 1, 3, 5, 10, and 14 of UV exposure) for quantification. Leaves were snap frozen, then stored at −80°C until used. They were then ground in liquid nitrogen using a mortar and pestle and 0.1 g leaf material was placed into micro-tubes with 1 mL acidified methanol (1% HCl, 20% H_2O, 79% CH_3OH (v/v)) before incubation in the dark at 4°C for 4 days. Absorbance was recorded at 330 nm using a spectrophotometer (Shimadzu UV/VIS 1800). Absorbance was normalized per leaf fresh weight. For each experiment, three plants per treatment were measured (one from each of the three replicated treatment OTFB boxes with accompanying control boxes) and in total three independent experiments were performed, that is $n = 9$. For control samples, $n = 18$.

TAC was analyzed using a commercially available kit (TAC Assay kit, Sigma-MAK187). Ground leaf tissue (0.1 g; see above) from the second true leaf was extracted in 1 mL of ice cold 1× phosphate-buffered saline (PBS) and following centrifugation, the supernatant was diluted 1:100 to bring values within range of kit standards. Samples were assayed according to the manufacturer's protocol, by comparing the absorbances of diluted extracts at 570 nm with Trolox standards and values normalized to tissue fresh weight. $n = 3$ for the UV-enriched treatments and $n = 6$ for the control treatment.

DNA damage detection

With replications as for flavonoid analysis, cyclobutane pyrimidine dimers were quantified using an immunoassay following the protocol from van de Poll et al. (2001). First, DNA was extracted from ground leaf tissue (see above) from the second true leaf from the base of the plant on days 1, 3, 5, 10, and 14 using the E.Z.N.A. Plant DNA Kit (Omega Bio-Tek, GA, USA), and dissolved in 100 µL TE buffer (pH 8.0). The DNA concentration was determined fluorometrically in a microplate reader (GENius, Tecan, Salzburg, Austria) using the Quantifluor dye (Promega, Madison, WI, USA). Of each sample, 50 ng DNA was used for the Southern blot. CPDs were subsequently labeled on the membrane by using a primary antibody against CPDs produced in mouse (H3 clone 4F6, Sigma Aldrich, St. Louis,

MO, USA). Detection was conducted by peroxidase coupled to the secondary antibody (Anti-Mouse IgG (whole molecule)-Peroxidase, Sigma Aldrich) using an enhanced chemiluminescent substrate (Pierce ECL, Thermo Fisher Scientific, Waltham, MA, USA). On each blot, a CPD calibration standard was included to allow absolute quantification of CPDs Mb^{-1} (Pescheck et al., 2014).

Plant hormone analysis

The second true leaves from the base of the plant were harvested on days 3 and 5. Leaves from three different plants within one experiment were pooled to obtain approximately 300 mg material. Leaf tissues were snap frozen in liquid nitrogen and kept at −80°C. All samples were then ground with a mortar and pestle in liquid nitrogen and again kept at −80°C until used. In total, three independent experiments generated three replicates. Each pooled sample was subdivided in separate 100 mg fractions for the extraction of the different hormone groups.

Auxin and ABA analysis

Samples were extracted in 500 µL of 80% v/v methanol. [C^{13}]-IAA (100 pmol, (phenyl-$^{13}C_6$)-indole-3-acetic acid, 99%, Cambridge Isotopes, Tewksbury, MA, USA) and D6-ABA (150 pmol, [$^2H_6$](+)-cis, trans-abscisic acid, [(S)-5-[$^2H_6$](1-hydroxy-2,6,6-trimethyl-4-oxocyclohex-2-en-1-yl)-3-methyl-(2Z,4E)-pentadienoic acid], Olchemim, Olomouc, Czech Republic) were added as internal tracers. After overnight extraction, samples were centrifuged (20 min, 15,000 g, 4°C, in an Eppendorf 5810R centrifuge, Eppendorf, Hamburg, Germany) and the supernatants were aliquoted in two equal parts. One aliquot was acidified using 5.0 mL of 6.0% v/v formic acid and loaded on a reversed-phase (RP)-C18 cartridge (500 mg, BondElut Varian, Middelburg, The Netherlands). The compounds of interest (IAA, ABA, and the oxidation products IAA-OX, IAA-OH, IBA-OX, and IBA-OH) were eluted with 5.0 mL of diethyl ether and dried under a nitrogen stream (TurboVap LV Evaporator, Zymark, New Boston, MA, USA). The remaining aliquot was hydrolyzed in 7.0 M NaOH for 3 h at 100°C under a water-saturated nitrogen atmosphere. After hydrolysis, the samples were acidified using 2.0 M HCl, desalted on an RP-C18 cartridge (500 mg), and eluted with diethyl ether. All samples were methylated using ethereal diazomethane to improve analysis sensitivity. Samples were analyzed using an Acquity UPLC system linked to a TQD triple quadrupole detector (Waters, Milford, MA, USA) equipped with an electrospray interface in positive mode. Samples (6.0 µL) were injected on an Acquity UPLC BEH C18 RP column (1.7 µm, 2.1 × 50 mm, Waters) using a column temperature of 30°C and eluted at 0.3 mL min^{-1} with the following gradient of 0.01 M ammonium acetate (solvent A) and methanol (solvent B): 0 – 2 min isocratic 90/10 A/B and 2 – 4 min linear gradient to 10/90 A/B. Quantitative analysis was obtained by multiple reactant monitoring of selected transitions based on the MH^+ ion (dwell time 0.02 s) and the most appropriate compound-specific product ions in combination with the compound-specific cone and collision settings. All data were processed using Masslynx/Quanlynx software V4.1 (Waters). Data are expressed in picomoles per gram fresh weight (pmol g^{-1} FW).

Gibberellin analysis

Samples were extracted overnight in 500 µL acidified methanol pH 4.0 (80/20, methanol/5.0 mM formic acid-containing butylated hydroxytoluene (3 – 5 crystals)). As internal tracers, D_2-GA1 ($C_{19}H^2_{22}H_2O_6$), D_2-GA4 ($C_{19}H^2_{22}H_2O_5$), D_2-GA8 ($C_{19}H^2_{22}H_2O_7$), D_2-GA9 ($C_{19}H^2_{22}H_2O_4$), D_2-GA15 ($C_{20}H^2_{24}H_2O_4$), D_2-GA19 ($C_{20}H^2_{24}H_2O_6$), D_2-GA20 ($C_{19}H^2_{22}H_2O_5$), and D_2-GA29 ($C_{19}H^2_{22}H_2O_6$; 20 pmol each, Olchemim) were added. After purification on an RP-C18 cartridge (500 mg) as described above for auxins, samples were derivatized with *N*-(3-dimethylaminopropyl)-*N*′-ethylcarbodiimide hydrochloride (Sigma–Aldrich, 1.0 mg per sample, pH 4.0, 60 min, 37°C under continuous shaking in an Eppendorf thermomixer) and analyzed using a UPLC–MS/MS equipped with an electrospray interface in positive mode (ACQUITY, TQD, Waters). Samples (6.0 µL, partial loop mode using a 10 µL sample loop) were injected on an ACQUITY BEH C18 column (2.1 × 50 mm; 1.7 mm, Waters) using a column temperature of 30°C and eluted at 450 µL min^{-1} with the following gradient of 0.1% v/v formic acid in water (solvent A) and 0.1% v/v formic acid in acetonitrile (solvent B): 0 – 0.8 min isocratic 92/8 A/B; 0.8 – 5 min linear gradient to 60/40 A/B; and 5 – 5.5 min linear gradient to 10/90 A/B. Quantitative analysis was performed by multiple reactant monitoring of selected transitions based on the MH^+ ion (dwell time 0.02 s) and the most appropriate compound-specific product ions in combination with the compound-specific cone and collision settings. Transitions are grouped in specific time windows according to the compound-specific retention time in order to keep the dwell time at 0.02 s. All data were processed using Masslynx/Quanlynx software V4.1 (Waters). Data are expressed in picomoles per gram fresh weight (pmol g^{-1} FW).

Statistical analysis

Statistical analysis was performed using either SPSS 19.0 (IBM, Armonk, NY, USA), STATA 14.0 or Wizard for Macintosh (App Store, Apple Inc., Cupertino, CA, USA). Morphological parameters (Figures 1–5) were analyzed using error propagation where the standard deviations of the ratios were approximated using Taylor linearization (Taylor, 1997) as further described in Qian et al. (2020), and tests of differences between means due to treatment (UV-A, UV-B, or control) were performed using analysis of variance (ANOVA). Paired *T* tests were used to test for changes in length of first–seventh petioles and parameters related to the second–fourth true leaves (Figures 2–4 and Tables 1, 2). Paired *T* test was also used for evaluating significant changes in each of LAEFC, TUAP, and TAC (Figure 8 and Supplementary Table S1). For data generated at different time periods of UV exposure, including analysis of chlorophyll fluorescence, chlorophyll content of the first true leaf,

and DNA dimer, two-way ANOVA was performed to test whether each variable was significantly affected by treatment or time of UV exposure. For data including chlorophyll fluorescence and chlorophyll content of the youngest well-developed leaf, and plant hormone concentration, *T* tests were performed to analyze if the differences between UV-exposed and control samples were significant or not.

To describe the relationship between the LAEFC and TUAP measurements, a simple regression model was first fitted. Thereafter, additional explanatory variables giving number of days of treatment/leaf age and two dummy variables taking into account treatment (UV-A-enriched, UV-B-enriched, and control) were included, to see if they would contribute in describing the dependent variable LAEFC. The final model included the TUAP variable and the variable days of treatment as explanatory variables. The residuals were analyzed and the assumptions behind the model seemed to be fulfilled, and showed no signs of systematic pattern, supporting the choice of model.

The same approach was used when TAC was the dependent variable and as explanatory variables in the full model; TUAP, days of treatment, two dummy variables for the treatment (UV-A, UV-B, and control). The final model included the same explanatory variables as the first model, TUAP and days of treatment, the other explanatory variables were not significant, thereby not contributing to the explanation of the values of TAC. The analysis of the residuals did not show any indication on deviations from the model assumptions.

Supplemental data

The following materials are available in the online version of this article.

Supplemental Table S1. Pairwise *T* test for significance of treatment of cucumber seedlings

Supplemental Figure S1. Maximum photochemical efficiency (F_v/F_m) measured in cucumber plants grown under different light conditions.

Supplemental Figure S2. Time courses of photosynthetic parameters measured in cucumber plants grown under different light conditions.

Supplemental Figure S3. The monophasic relationship between LAEFC and TUAP.

Supplemental Figure S4. Residual (ε) plots for models of correlation between the three methods used to determine LAEFC, TUAP, and TAC.

Supplemental Figure S5. Average number of flowers in each leaf node in cucumber plants that had been exposed to UV-A-enriched, UV-B-enriched non-UV supplemented growth light as seedlings.

Funding

This research was supported by grants to Å.S. from the Knowledge Foundation (kks.se; contract no. 20130164) and the Swedish Research Council Formas (formas.se/en; Contract no. 942-2015-516). The Örebro University's Faculty for Business, Science and Technology also supported the research. M.A.K.J. acknowledges support by Science Foundation Ireland (S16/IA/4418). E.P. acknowledges support by the Flemish Science Foundation (FWO, grant G000515N). M.Q. was sponsored by the China Scholarship Council (CSC no. 201406320076).

Conflict of interest statement. None declared.

References

Adamse P, Britz SJ (1992) Amelioration of UV-B damage under high irradiance. I. Role of photosynthesis. Photochem Photobiol **56**: 645–650

Adamse P, Britz SJ, Caldwell CR (1994) Amelioration of UV-B damage under high irradiance. II. Role of blue-light photoreceptors. Photochem Photobiol **60**: 110–115

Agati G, Azzarello E, Pollastri S, Tattini M (2012) Flavonoids as antioxidants in plants: Location and functional significance. Plant Sci **196**: 67–76

Ballaré CL, Barnes PW, Kendrick RE (1991) Photomorphogenic effects of UV-B radiation on hypocotyl elongation in wild type and stable-phytochrome-deficient mutant seedlings of cucumber. Physiol Plant **83**: 652–658

Barnes PW, Ballaré CL, Caldwell MM (1996) Photomorphogenic effects of UV-B radiation on plants: consequences for light competition. J Plant Physiol **148**: 15–20

Barnes PW, Williamson CE, Lucas RM, Robinson SA, Madronich S, Paul ND, Bornman JF, Bais AF, Sulzberger B, Wilson SR, et al. (2019) Ozone depletion, ultraviolet radiation, climate change and prospects for a sustainable future. Nat Sustain **2**: 569–579

Barthod S, Cerovic Z, Epron D (2007) Can dual chlorophyll fluorescence excitation be used to assess the variation in the content of UV-absorbing phenolic compounds in leaves of temperate tree species along a light gradient? J Exp Bot **58**: 1753–1760

Bernhard GH, Neale RE, Barnes PW, Neale PJ, Zepp RG, Wilson SR, Andrady AL et al. (2020) Environmental effects of stratospheric ozone depletion, UV radiation and interactions with climate change: UNEP Environmental Effects Assessment Panel, update 2019. Photochem Photobiol Sci **19**: 542–584

Bornman JF, Barnes PW, Robson TM, Robinson SA, Jansen MAK, Ballaré CL, Flint SD (2019) Linkages between stratospheric ozone, UV radiation and climate change and their implications for terrestrial ecosystems. Photochem Photobiol Sci **18**: 681–716

Bouderias S, Teszlák P, Jakab G, Kőrösi L (2020) Age- and season-dependent pattern of flavonol glycosides in Cabernet Sauvignon grapevine leaves. Sci Rep **10**: 14241

Brodfuhrer U (1955) Der Einfluss einer abgestuften Dosierung von ultravioletter Sonnenstrahlung auf das Wachstum der Pflanzen. Planta **45**: 1–56

Csepregi K, Neugart S, Schreiner M, Hideg É (2016) Comparative evaluation of total antioxidant capacities of plant polyphenols. Molecules **21**: 208

Dickson JG, Caldwell M (1978) Leaf development of *Rumex patientia* L. (*Polygonaceae*) exposed to UV irradiation (280–320 nm). Am J Bot **65**: 857–863

Fukuda S, Satoh A, Kasahara H, Matsuyama H, Takeuchi Y (2008) Effects of ultraviolet-B irradiation on the cuticular wax of cucumber (*Cucumis sativus*) cotyledons. J Plant Res **121**: 179–189

Hayes S, Velanis CN, Jenkins GI, Franklin KA (2014) UV-B detected by the UVR8 photoreceptor antagonizes auxin signaling and plant shade avoidance. Proc Natl Acad Sci USA **111**: 11894–11899

He J-M, Ma X-G, Zhang Y, Sun T-F, Xu F-F, Chen Y-P, Liu X, Yue M (2013) Role and interrelationship of Gα protein, hydrogen peroxide, and nitric oxide in ultraviolet-B-induced stomatal closure in Arabidopsis leaves. Plant Physiol **161**: 1570–1583

Hectors K, van Oevelen S, Guisez Y, Prinsen E, Jansen MAK (2012) The phytohormone auxin is a component of the regulatory system

that controls UV-mediated accumulation of flavonoids and UV-induced morphogenesis. Physiol Plant **145**: 594–603.

Hideg É, Jansen MAK, Strid Å (2013) UV-B exposure, ROS and stress; inseparable companions *or* loosely linked associates? Trends Plant Sci **18**: 107–115

Hideg É, Strid Å (2017) The effects of UV-B on the biochemistry and metabolism in plants. *In* BR. Jordan, ed, UV-B Radiation and Plant Life: Molecular Biology to Ecology. CABI press, Oxford, UK, pp 90–110.

Jansen MAK, Bilger W, Hideg É, Strid Å; UV4 Plants Workshop Participants, Urban O (2019) Interactive effects of UV-B radiation in a complex environment. Plant Physiol Biochem **134**: 1–8

Jansen MAK, Bornman JF (2012) UV-B radiation: from generic stressor to specific regulator. Physiol Plant **145**: 501–504

Jansen MAK, Gaba V, Greenberg BM (1998) Higher plants and UV-B radiation: balancing damage, repair and acclimation. Trends Plant Sci **3**: 131–135

Jiang L, Wang Y, Björn LO, Li S (2011) UV-B-induced DNA damage mediates expression changes of cell cycle regulatory genes in Arabidopsis root tips. Planta **233**: 831–841

Jordan BR, Strid Å, Wargent JJ (2016) What role does UV-B play in determining photosynthesis? *In* Md, Pessarakli, ed., Handbook of Photosynthesis, Ed 3. CRC Press, Boca Raton, FL, pp 275–286

Kalbin G, Hidema J, Brosché M, Kumagai T, Bornman JF, Strid Å (2001) UV-B-induced DNA damage and expression of defence genes under UV-B stress: tissue-specific molecular marker analysis in leaves. Plant Cell Environ **24**: 983–990

Kang H-S, Hidema J, Kumagai T (1998) Effects of light environment during culture on UV-induced cyclobutyl pyrimidine dimers and their photorepair in rice (*Oryza sativa* L.). Photochem Photobiol **68**: 71–77.

Krizek DT (1978) Differential sensitivity of two cultivars of cucumber (*Cucumis sativus* L.) to increased UV-B irradiance. I. Dose–response studies. Final Report on Biological and Climatic Effects Research. USDA-EPA, Environmental Protection Agency, Washington, DC.

Krizek DT, Mirecki RM, Kramer GF (1994) Growth analysis of UV-B irradiated cucumber seedlings as influenced by photosynthetic photon flux source and cultivar. Physiol Plant **90**: 593–599

Krizek DT, Mirecki RM, Britz SJ (1997) Inhibitory effects of ambient levels of solar UV-A and UV-B radiation on growth of cucumber. Physiol Plant **100**: 886–893

Lake JA, Field KJ, Davey MP, Berrling DJ, Lomax BH (2009) Metabolomic and physiological responses reveal multi-phasic acclimation of *Arabidopsis thaliana* to chronic UV radiation. Plant Cell Environ **32**: 1377–1389

Liang T, Mei S, Shi C, Yang Y, Peng Y, Ma L, Wang F, Li X, Huang X, Yin Y, Liu H (2018) UVR8 interacts with BES1 and BIM1 to regulate transcription and photomorphogenesis in Arabidopsis. Dev Cell **44**: 512–523.e5

Liu F, Stützel H (2004) Biomass partitioning, specific leaf area, and water use efficiency of vegetable amaranth (*Amaranthus* spp.) in response to drought stress. Sci Horticult **102**: 15–27.

Majer P, Hideg É (2012) Developmental stage is an important factor that determines the antioxidant responses of young and old grapevine leaves under UV irradiation in a greenhouse. Plant Physiol Biochem **50**: 15–23

Martínez-Lüscher J, Morales F, Delrot S, Sánchez-Díaz M, Gomés E, Aguirreolea J, Pascual I (2013) Short- and long-term physiological responses of grapevine leaves to UV-B radiation. Plant Sci **213**: 114–122

Morales LO, Brosché M, Vainonen J, Jenkins GI, Wargent JJ, Sipari N, Strid Å, Lindfors AV, Tegelberg R, Aphalo PJ (2013) Multiple roles for UV RESISTANCE LOCUS8 in regulating gene expression and metabolite accumulation in Arabidopsis under solar ultraviolet radiation. Plant Physiol **161**: 744–759

Morgenstern A, Ekholm A, Scheewe P, Rumpunen K (2014) Changes in content of major phenolic compounds during leaf development of sea buckthorn (*Hippophaë rhamnoides* L.). Agricult Food Sci **23**: 207–219

Murali NS, Teramura AH (1986) Intraspecific differences in *Cucumis sativus* sensitivity to ultraviolet-B radiation. Physiol Plant **68**: 673–677

Murchie EH, Lawson T (2013) Chlorophyll fluorescence analysis: a guide to good practice and understanding some new applications. J Exp Bot **64**: 3983–3998

Paik I, Huq E (2019) Plant photoreceptors: Multi-functional sensory proteins and their signaling networks. Semin Cell Dev Biol **92**: 114–121

Pescheck F, Lohbeck KT, Roleda MY, Bilger W (2014) UVB induced DNA and photosystem II damage in two intertidal green macroalgae: distinct survival strategies in UV-screening and non-screening *Chlorophyta*. J Photochem Photobiol B Biol **132**: 85–93

Potters G, Pasternak TP, Guisez Y, Palme KJ, Jansen MAK (2007) Stress-induced morphogenic responses: growing out of trouble? Trends Plant Sci **12**: 98–105

Qaderi MM, Yeung EC, Reid DM (2008) Growth and physiological responses of an invasive alien species, *Silene noctiflora*, during two developmental stages to four levels of ultraviolet-B radiation. Ecoscience **15**: 150–159.

Qian M, Kalbina I, Rosenqvist E, Jansen MAK, Teng Y, Strid Å (2019) UV regulates expression of phenylpropanoid biosynthesis genes in cucumber (*Cucumis sativus* L.) in an organ and spectrum dependent manner. Photochem Photobiol Sci **18**: 424–433

Qian M, Rosenqvist E, Flygare A-M, Kalbina I, Teng Y, Jansen MAK, Strid Å (2020) UV-A light induces a robust and dwarfed phenotype in cucumber plants (*Cucumis sativus* L.) without affecting fruit yield. Sci Horticult **263**: 109110

Radziejwoski A, Vlieghe K, Lammens T, Berckmans B, Maes S, Jansen MAK, Knappe C, Albert A, Seidlitz HK, Bahnweg G, et al. (2011) Atypical E2F activity coordinates PHR1 photolyase gene transcription with endoreduplication onset. EMBO J **30**: 355–363

Rai N, Neugart S, Yan Y, Wang F, Siipola SM, Lindfors AV, Winkler JB, Albert A, Brosché M, Lehto T, et al. (2019) How do cryptochromes and UVR8 interact in natural and simulated sunlight? J Exp Bot **70**: 4975–4990

Rai N, O'Hara A, Farkas D, Safronov O, Ratanasopa K, Siipola S, Wang F, Lindfors A, Sipari N, Jenkins GI, et al. (2020) The photoreceptor UVR8 mediates the perception of both UV-B and UV-A wavelengths up to 350 nm of sunlight with responsivity moderated by cryptochromes. Plant Cell Environ **43**: 1513–1527

Rai N, Morales LO, Aphalo PJ (2021) Perception of solar UV radiation by plants: photoreceptors and mechanisms. Plant Physiol **187**: 1382–1396

Reifenrath K, Müller C (2007) Species-specific and leaf-age dependent effects of ultraviolet radiation on two Brassicaceae. Phytochemistry **68**: 875–885

Robson TM, Hartikainen SM, Aphalo PJ (2015a) How does solar ultraviolet-B radiation improve drought tolerance of silver birch (*Betula pendula* Roth.) seedlings? Plant Cell Environ **38**: 953–967

Robson TM, Klem K, Urban O, Jansen MAK (2015b) Re-interpreting plant morphological responses to UV-B radiation. Plant Cell Environ **38**: 856–866

Rodríguez-Calzada T, Qian M, Strid Å, Neugart S, Schreiner M, Torres-Pacheco I, Guevara-Gonzales R (2019) Effect of UV-B radiation on morphology, phenolic compound production, gene expression, and subsequent drought stress responses in chili pepper (*Capsicum annuum* L.). Plant Physiol Biochem **134**: 94–102

Sävenstrand H, Brosché M, Strid Å (2004) Ultraviolet-B signalling: Arabidopsis brassinosteroid mutants are defective in UV-B regulated defence gene expression. Plant Physiol Biochem **42**: 687–694

Sharma A, Sharma B, Hayes S, Kerner K, Hoecker U, Jenkins GI, Franklin KA (2019) UVR8 disrupts stabilisation of PIF5 by COP1 to inhibit plant stem elongation in sunlight. Nat Commun **10**: 4417

Shinkle JR, Edwards MC, Koenig A, Shaltz A, Barnes PW (2010) Photomorphogenic regulation of increases in UV-absorbing

pigments in cucumber (*Cucumis sativus*) and *Arabidopsis thaliana* seedlings induced by different UV-B and UV-C wavebands. Physiol Plant **138**: 113–121

van de Poll WH, Eggert A, Buma AGJ, Breeman AM (2001) Effects of UV-B-induced DNA damage and photoinhibition on growth of temperate marine red macrophytes: habitat-related differences in UV-B tolerance. J Phycol **37**: 30–37

Van de Staaij JWM, Bolink E, Rozema J, Ernst WHO (1997) The impact of elevated UV-B (280–320 nm) radiation levels on the reproduction biology of a highland and a lowland population of *Silene vulgaris*. Plant Ecol **128**: 173–179

Vanhaelewyn L, Prinsen E, Van Der Straeten D, Vandenbussche F (2016) Hormone-controlled UV-B responses in plants. J Exp Bot **67**: 4469–4482

Takeuchi Y, Kubo H, Kasahara H, Sasaki T (1996) Adaptive alterations in the activities of scavengers of active oxygen in cucumber cotyledons irradiated with UV-B. J Plant Physiol **147**: 589–592

Taylor JR (1997) An introduction to error analysis. *In* The Study of Uncertainties in Physical Measurements, Ed 2. University Science Books, Sausalito, CA.

Tossi V, Lamattina L, Jenkins GI, Cassia RO (2014) Ultraviolet-B-induced stomatal closure in Arabidopsis is regulated by the UV RESISTANCE LOCUS8 photoreceptor in a nitric oxide-dependent mechanism. Plant Physiol **164**: 2220–2230

Wargent JJ, Gegas VC, Jenkins GI, Doonan JH, Paul ND (2009) UVR8 in *Arabidopsis thaliana* regulates multiple aspects of cellular differentiation during leaf development in response to ultraviolet B radiation. New Phytol **183**: 315–326

Yamasaki S, Shimada E, Kuwano T, Kawano T, Noguchi N (2010) Continuous UV-B irradiation induces endoreduplication and peroxidase activity in epidermal cells surrounding trichomes on cucumber cotyledons. J Radiat Res **51**: 187–196

Yamasaki S, Shigeto H, Ashihara Y, Noguchi N (2014) Continuous long-term UV-B irradiation reduces division and expansion of epidermal cells in true leaves but accelerates developmental stages such as true leaf unfolding and male flower bud production in cucumber (*Cucumis sativus, L.) seedlings*. Environ Control Biol **52**: 13–19.

Yu S-G, Björn LO (1997) Effects of UVB radiation on light-dependent and light-independent protein phosphorylation in thylakoid proteins. J Photochem Photobiol B Biol **37**: 212–218